
Ensemble Adversarial Training: Attacks and Defenses

Florian Tramèr¹, Alexey Kurakin², Nicolas Papernot³,
 Dan Boneh¹, and Patrick McDaniel³

¹Stanford University, ²Google Brain, ³Pennsylvania State University

Abstract

Machine learning models are vulnerable to *adversarial examples*, inputs maliciously perturbed to mislead the model. These inputs *transfer* between models, thus enabling *black-box* attacks against deployed models. *Adversarial training* increases robustness to attacks by injecting adversarial examples into training data. Surprisingly, we find that although adversarially trained models exhibit strong robustness to some white-box attacks (i.e., with knowledge of the model parameters), they remain highly vulnerable to *transferred* adversarial examples crafted on other models. We show that the reason for this vulnerability is the model’s decision surface exhibiting sharp curvature in the vicinity of the data points, thus hindering attacks based on first-order approximations of the model’s loss, but permitting black-box attacks that use adversarial examples transferred from another model. We harness this observation in two ways: First, we propose a simple yet powerful novel attack that first applies a small *random* perturbation to an input, before finding the optimal perturbation under a first-order approximation. Our attack outperforms prior “single-step” attacks on models trained with or without adversarial training. Second, we propose *Ensemble Adversarial Training*, an extension of adversarial training that additionally augments training data with perturbed inputs transferred from a number of fixed pre-trained models. On MNIST and ImageNet, ensemble adversarial training vastly improves robustness to black-box attacks.

1 Introduction

Machine learning (ML) models are often vulnerable to *adversarial examples*, maliciously perturbed inputs designed to mislead a model at test time [2, 19, 5, 14]. Adversarial examples are a security threat to practical deployment of ML systems. Notably, Szegedy et al. [19] showed that these inputs *transfer* (or generalize) across models, thus enabling *black-box* attacks on deployed models [13, 9]: an adversary can train a local model (possibly by issuing prediction queries to the target model [13, 21]), find an adversarial example on the local model, and apply it to attack the target model.

Szegedy et al. [19] proposed to increase a model’s robustness by injecting adversarial examples into training data. Adversarially trained models often gain resilience to “one-shot” attacks, i.e., perturbations obtained by taking a single step along the gradient of the model’s loss [5, 8], but remain vulnerable to stronger attacks that iteratively maximize the model’s loss [10, 8]. Because these stronger attacks fail to reliably transfer between models [8], one might conclude that adversarial training successfully defends against adversaries limited to black-box interaction with the target model. We show that this is not the case.

Robustness of adversarial training to black-box attacks has not been studied extensively. Goodfellow et al. [5] reported that an adversarially trained maxout network on MNIST has slightly higher error rate on transferred examples than on examples crafted from the model itself. Papernot et al. [13] found that a model trained on small perturbations can be evaded by transferring larger perturbations from another model. We show that adversarially trained models on MNIST and ImageNet are *significantly*

more robust to adversarial examples computed on the model itself (i.e., a white-box attack), than to transferred examples computed *using the same method* on another model (i.e., a black-box attack).

This situation is paradoxical, as white-box attacks correspond to a *stronger* threat model than black-box attacks. We show that this discrepancy is due to the loss function of an adversarially trained model exhibiting sharp curvature in the vicinity of the data points, thus rendering attacks based on first-order approximations of the model’s loss inaccurate. A similar phenomenon, commonly referred to as *gradient masking* [15], is known to affect other defenses against adversarial examples, such as distillation [16, 4] and saturating networks [11, 3]. We therefore strongly *advise researchers to always include evaluations of future defensive strategies on transferred adversarial examples*.

We harness our observations in two ways. First, we introduce a simple yet powerful attack that combines a small *random* perturbation of the input—in order to escape the non-smooth vicinity of the data point—and a *single* step in the direction of the gradient of the model’s loss function. While seemingly weaker than the Fast Gradient Sign Method of Goodfellow et al. [5], our attack significantly outperforms it for a same perturbation norm, for models trained with or without adversarial training.

Second, we propose *Ensemble Adversarial Training*, a training methodology that incorporates perturbed inputs crafted both on the trained model, as well as on a number of *pre-trained models*. Intuitively, our approach *decouples* adversarial example generation from the parameters of the model being trained to ensure that this model is evaluated on perturbations that are “hard” to classify throughout training. We evaluate our technique on MNIST and ImageNet (for Inception v3 and Inception ResNet v2 models [17]). Despite a small decrease in accuracy on clean inputs and white-box attacks (compared to standard adversarial training), we significantly increase robustness to adversarial examples transferred from an independent model *held out during training*. While training models to be robust to all *white-box* attacks appears out-of-reach using current techniques [8], our work gives promising new directions and results towards securing ML systems against *black-box* adversaries.

Contributions: In summary, our work makes the following contributions:

- We show that the robustness of adversarially trained models to white-box “one-shot” attacks is misleading, as it is partly due to *local artifacts* of the model’s decision surface. We find that these models remain highly vulnerable to transferred perturbations (Section 3).
- We introduce a new white-box attack where we first perturb the data point to escape the non-smooth region around that point, then build an adversarial example from this perturbed point. Our attack outperforms other one-shot methods on all models we trained (Section 4).
- We propose *Ensemble Adversarial Training*, a training methodology that incorporates adversarial examples transferred from *other pre-trained models*. On MNIST and ImageNet, our method significantly increases robustness to black-box attacks, where adversarial examples are transferred from a different model held out during training (Section 5).

2 Background and Related Work

We first introduce some notation. We use x and y_{true} to denote an input from the domain $[0, 1]^d$ and its label. An adversarial example computed by perturbing x is denoted x^{adv} . The norm of the perturbation (always in the ℓ_∞ norm [5]) is denoted ϵ . For an ML model f , we denote the model’s estimate of the probability $p(y | x)$ as $f_y(x)$. The loss function used to train the model is $J(x, y)$.

2.1 Threat Model

We consider attacks mounted with adversarial examples [19, 2] to mislead a ML model at test time. For an input x (with label y_{true}) and a target model f , an adversary tries to find an adversarial input x^{adv} (created by adding a perturbation of small ℓ_∞ norm to x [5]) such that $f(x^{adv}) \neq y_{\text{true}}$.

We distinguish between *white-box* adversaries that have access to the target model’s weights, and *black-box* adversaries that only interact with a model’s prediction interface. Formal definitions for these adversaries are in Appendix A. Although security against white-box attacks is the stronger notion (and the one we ideally want ML models to achieve), black-box security is a reasonable and more tractable goal for ML models deployed in adversarial environments, where unauthorized access to the model is likely to be prevented via traditional security mechanisms. We focus on “non-adaptive” black-box adversaries that attack a model by *transferring* adversarial examples crafted from a local model, trained without interacting with the target. We discuss adaptive black-box attacks in Section 6.

2.2 Adversarial Example Generation Algorithms

We consider three algorithms to generate adversarial examples. The first two are *one-shot* (i.e., they require a single gradient computation); the third is *iterative*—it computes multiple gradient updates. For all attacks, we enforce that $x^{adv} \in [0, 1]^d$ by clipping all components of x^{adv} .

Fast Gradient Sign Method (FGSM): This method [5] finds perturbations with a fixed ℓ_∞ -norm:

$$x^{adv} = x + \varepsilon \cdot \text{sign}(\nabla_x J(x, y_{true})) .$$

The FGSM is easy to compute and thus particularly amenable to *adversarial training* (see Section 2.3).

Targeted FGSM: This FGSM variant aims at fooling a model into outputting a given target class:

$$x^{adv} = x - \varepsilon \cdot \text{sign}(\nabla_x J(x, y_{target})) .$$

As in [7, 8], we use as target the *least-likely* class predicted by the network, $y_{target} = \arg \min_y \{f_y(x)\}$.

Iterative FGSM (I-FGSM): This method iteratively applies the FGSM k times with budget $\epsilon' = \epsilon/k$. The I-FGSM usually induces higher error rates than the FGSM (for fixed ϵ) [7, 8]. Yet, I-FGSM samples *transfer* across models at lower rates and thus produce weaker black-box attacks [8].

2.3 Adversarial Training

Adversarial training aims at increasing model robustness by injecting adversarial examples into the training set [19, 5]. We consider two variants. For models without batch normalization [6], we use the objective of Goodfellow et al. [5]: the model is evaluated on the clean input and FGSM example for each batch input. For models with batch normalization, Kurakin et al. [8] obtain better results when half the inputs in each batch are *replaced* by adversarial examples. Kurakin et al. [8] suggest not to use the true label y_{true} in the FGSM due to *label leaking*: the model learns to recognize perturbations associated with a label. On MNIST, we thus compute the FGSM using the model’s prediction $\arg \max_i (f_i(x))$ in lieu of y_{true} , and on ImageNet, we use the targeted FGSM as in [8].

2.4 Gradient Masking

Many defenses against adversarial examples are more robust to *white-box* attacks (e.g., those in Section 2.2) than to *black-box* attacks, where perturbed inputs are transferred from another model [15]. This is due to *gradient masking* [13, 15]: defenses leave decision boundaries mostly untouched but damage the gradient used in white-box attacks. For example, *Distillation* [16] and *Saturating Networks* [11] introduce numerical instabilities in gradient computations [4, 3] (see Appendix C).

Prior work has alluded that adversarial training (on MNIST) may also exhibit a gap in robustness to white-box and black-box attacks. Goodfellow et al. [5] report that an adversarially trained model is slightly more robust to FGSM samples computed on the model itself, than to samples transferred from another model. Papernot et al. [13] show that a model trained on perturbations with small norm is vulnerable to larger transferred perturbations. Tramèr et al. [20] find that adversarial training fails to sufficiently displace a model’s decision boundary to prevent adversarial examples from transferring.

3 Black-Box Attacks Against Adversarial Training

In this section, we show that adversarial training on MNIST and ImageNet exhibits a *large* gap between robustness to white-box and black-box attacks. We explain this by a gradient masking effect: The defended model’s loss function is non-smooth in the vicinity of data points, thus rendering a first-order approximation of the loss inaccurate. The observed robustness of adversarially trained models to white-box “one-shot” attacks (such as the FGSM) is therefore partly due to *local* artifacts of the model’s decision surface. In Section 4, we harness this observation to build a novel *one-shot* attack that vastly outperforms the FGSM on models trained with or without adversarial training.

3.1 Experimental Setup

MNIST: We train two different convolutional networks (denoted A and B in Table 6 in the Appendix) on MNIST. For architecture A, we also train a model A_{adv} using adversarial training. Specifically, A_{adv} is trained for 6 epochs on batches of 64 clean samples and 64 FGSM samples with $\epsilon = 0.3$.

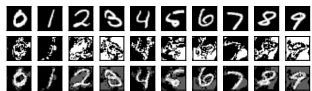
Table 1: **Error rates (in %) of adversarial examples transferred between models.** We use the FGSM with $\epsilon = 0.3$ for MNIST and $\epsilon = 16/256$ (targeted at the least-likely class) for ImageNet. Diagonal elements correspond to a white-box attack. Results on MNIST are computed over the full test set; results on ImageNet use a random sample of 10,000 inputs from the test set. Note that black-box attacks are more successful when the source and target models have different architectures.

Source Model	Target Model			Source Model	Target Model			Source Model	Target Model		
	A	A_{adv}	B		v3	$v3_{\text{adv}}$	v4		v3	$v3_{\text{adv}}$	v4
A	71.4	11.9	50.7	v3	69.7	35.8	39.2	v3	42.8	13.4	15.0
A_{adv}	24.7	3.6	25.4	$v3_{\text{adv}}$	36.4	26.8	31.1	$v3_{\text{adv}}$	13.0	9.0	10.3
B	62.4	18.2	84.6	v4	43.8	36.5	60.2	v4	18.8	13.5	30.8

MNIST

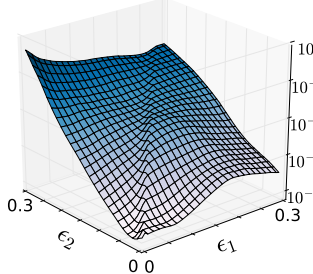


(a) Model A.

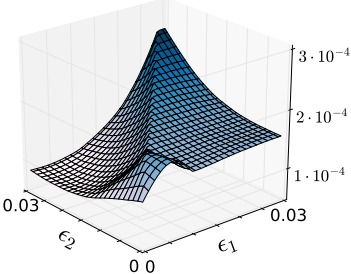


(b) Model A_{adv} .

ImageNet (top 1)



(a) Loss of model A_{adv} (log-scale).



(b) Zoom in for small ϵ_1, ϵ_2 .

Figure 2: **Illustration of gradient masking for adversarial training on MNIST.** We plot the loss of model A_{adv} on points of the form $x^* = x + \epsilon_1 \cdot \text{sign}(g_1) + \epsilon_2 \cdot \text{sign}(g_2)$, where g_1 is the gradient of model A_{adv} and g_2 is the gradient of model B. Plot (b) is a zoomed version of (a) in the vicinity of the data point.

ImageNet: We use three different models: (1) An Inception v4 model [17]; (2) An Inception v3 model [18]; and (3) the adversarially trained Inception v3 model from [8], denoted $v3_{\text{adv}}$. Adversarial training follows the setup in [8] using synchronous distributed training on 50 machines, with mini-batches of 32 inputs per machine. We replace half of the inputs in each minibatch by FGSM examples (targeted at the least-likely class), with $\epsilon \in [0, \frac{16}{256}]$ sampled from a truncated normal distribution.

3.2 Vulnerability to Black-Box Attacks

We show that the adversarially trained Inception v3 model from Kurakin et al. [8] is more robust to white-box FGSM samples than to transferred FGSM samples. We report similar results on MNIST, corroborating observations of Goodfellow et al. [5]. For all pairs of models, we compute adversarial examples on one model (the source) and transfer them to the other (the target). When the source and target are the same, this corresponds to a white-box attack. For MNIST, we use $\epsilon = 0.3$ and for ImageNet we use $\epsilon = 16/256 \approx 0.06$. The results in Table 1 show that adversarial training greatly increases robustness to perturbations crafted on the model itself (i.e., white-box attacks). Although adversarial training also increases robustness to transferred examples, the error rate in a black-box setting is significantly higher than in a white-box setting. Thus, the apparent gain in robustness observed when evaluating adversarially trained models in isolation is misleading. Given the ubiquity of this pitfall among proposed defenses against adversarial examples [4, 3, 15], we advise researchers to *always consider both white-box and black-box adversaries when evaluating defensive strategies*.

3.3 Explaining Gradient Masking in Adversarial Training

We now show that the misleading robustness of adversarially trained models to white-box attacks is due to gradient masking. We find that the model’s loss function is non-smooth around data points, which renders first-order approximations inaccurate. In Appendix D, we discuss other hypotheses for gradient masking in adversarial training that however failed to be corroborated by our experiments.

Table 2: **Error rates (in %) for FGSM and RAND+FGSM samples.** On MNIST, we use $\epsilon = 0.3, \alpha = 0.05$. On ImageNet, we use $\epsilon = 16/256, \alpha = 8/256$. Results on MNIST are computed over the full test set; on ImageNet, we use a random sample of 10,000 inputs from the test set.

	A	A_{adv}	B	v3	$v3_{\text{adv}}$	v4	v3	$v3_{\text{adv}}$	v4
FGSM	71.4	3.6	84.6	69.7	26.8	60.2	42.8	9.0	30.8
RAND+FGSM	75.3	34.1	86.2	80.1	64.3	70.3	57.7	37.2	42.5
MNIST				ImageNet (top 1)				ImageNet (top 5)	

Easy Perturbations and Local Loss Curvature. The results in Table 1 reveal that adversarial examples computed on the adversarially trained models are actually “easy” to classify for all models. That is, perturbations crafted using model A_{adv} or $v3_{\text{adv}}$ as source transfer at lower rates, compared to when the source model is not adversarially trained. We visualize these easy perturbations by plotting the signed gradients and perturbed images for two MNIST models in Figure 1. As observed in [5], the gradients of adversarially trained models are very localized. In many cases, the perturbation traces out the digit and thus simply dampens the original signal. Remarkably, if we apply the FGSM with $\epsilon = 1$ (i.e., the clean image is fully replaced by the gradient), model A_{adv} retains 43% accuracy. Thus, the adversarially trained model often correctly classifies an input solely from the computed gradient.

We further visualize the evolution of the model’s loss function when inputs are perturbed. More precisely, Figure 2 plots the loss incurred by model A_{adv} when evaluated on examples of the form $x^* = x + \epsilon_1 \cdot \text{sign}(g_1) + \epsilon_2 \cdot \text{sign}(g_2)$, where g_1 is the gradient of model A_{adv} and g_2 is the gradient of model B. The point x was selected such that the FGSM sample computed on model B is misclassified by model A_{adv} (i.e., the adversarial example transfers). We see that the loss varies very little when moving along the signed gradient of A_{adv} , but the signed gradient of model B yields an adversarial input. However, in the vicinity of the data point, the situation is reversed: the loss increases sharply in the direction of the signed gradient of model A_{adv} . Thus, one-shot attacks on adversarially trained models produce perturbations that are overfit to the local shape of the models loss. The sharp increase in loss observed for small perturbations (see Figure 2 (b)) corroborates results of Kurakin et al. [8], who find that sometimes FGSM attacks with smaller ϵ succeed with *higher* probability. Additional illustrations are in Figure 3 in the Appendix.

4 A New Randomized One-Shot Attack

We exploit the observations above to create a one-shot attack that is more effective against adversarially trained models. We significantly increase the power of the FGSM if we apply a small *random* perturbation, to “escape” the non-smooth vicinity of the data point, before computing the gradient. Our new attack, called RAND+FGSM, is defined as follows, for parameters ϵ and α (where $\alpha < \epsilon$):

$$\begin{aligned} x' &= x + \alpha \cdot \text{sign}(\mathcal{N}(\mathbf{0}^d, \mathbf{I}^d)) \\ x^{\text{adv}} &= x' + (\epsilon - \alpha) \cdot \text{sign}(\nabla_{x'} J(x', y_{\text{true}})) . \end{aligned}$$

We can similarly define a RAND+FGSM variant targeted at the least likely class. Note that this attack remains “one-shot”, i.e., it requires a single gradient computation. The RAND+FGSM is thus a computationally efficient alternative to iterative methods (e.g., I-FGSM or the L-BFGS attack from [19]) that usually have higher success rates than FGSM for a given perturbation magnitude.

Experiments. We experimented with $\epsilon = 0.3, \alpha = 0.05$ on MNIST, and $\epsilon = 16/256, \alpha = 8/256$ on ImageNet for the targeted attack variant. Error rates for all models are in Table 2. Surprisingly, the RAND+FGSM outperforms the FGSM for all models. This suggests that for all models, the loss function is less smooth in the vicinity of data points. Note that simply using the FGSM with norm $\epsilon - \alpha$ yields a weaker attack than the FGSM with norm ϵ on all models.

We find that RAND+FGSM samples transfer at lower rates than FGSM examples (see Table 8 in the Appendix). Similar results were obtained for iterative attacks on ImageNet [8]. We also tried adversarial training using RAND+FGSM on MNIST, but were not able to increase robustness to either RAND+FGSM examples or FGSM examples (in white-box or black-box settings). Achieving robustness against the large class of RAND+FGSM perturbations may require novel techniques. However, as for iterative attacks, the fact that these strong attacks do not transfer at high rates implies that security against black-box adversaries remains an interesting goal.

Table 3: **Models used for ensemble adversarial training.** MNIST models are described in Appendix B. The pre-trained ResNet v2 [17] is limited to 50 layers. IncRes stands for Inception-ResNet.

	Trained Model	Pre-trained Models	Holdout Model
MNIST	A ($A_{adv\text{-}ens}$)	A, C, D	B
ImageNet	Inception v3 ($v3_{adv\text{-}ens3}$)	Inception v3, ResNet v2	Inception v4
	Inception v3 ($v3_{adv\text{-}ens4}$)	Inception v3, ResNet v2, IncRes v2	Inception v4
	IncRes v2 (IncRes v2 _{adv-ens})	Inception v3, IncRes v2	Inception v4

5 Ensemble Adversarial Training

In Section 3.3, we showed that gradients of adversarially trained models point in directions that produce easy perturbations. As a result, although the model appears robust when evaluated on white-box “one-shot” attacks, it remains vulnerable to adversarial examples transferred from other models. In this section, we first show why the *adversarial training objective* fails to prevent this form of gradient masking. We then introduce *Ensemble Adversarial Training*, a training technique that incorporates perturbations transferred from other models, to increase robustness to black-box attacks.

5.1 Avoiding Degenerate Minima of the Adversarial Training Objective.

Following [5], the loss \tilde{J} minimized during training consists of two weighted terms:

$$\tilde{J}(x, y_{true}) = \alpha \cdot J(x, y_{true}) + (1 - \alpha) \cdot J(x^{adv}, y_{true}),$$

where x^{adv} is the FGSM sample computed from x . Note that the adversarial loss term $J(x^{adv}, y_{true})$ admits (at least) two widely different global minima: (1) The model has no adversarial examples (i.e., the loss is low for all points in the ϵ -ball centered at x); (2) The model is the same as an undefended model, except that its gradient points into a non-adversarial direction. Our experiments suggest that adversarial training converges to a solution closer to this second *degenerate* minimum. Note that the training objective provides no means for “escaping” such minima: Once a model’s gradients produce easy adversarial examples, the adversarial loss has a limited influence on the training objective.

We introduce an extension of adversarial training designed to avoid these pitfalls. Our main idea is to *decouple* the generation of adversarial examples from the parameters of the model being trained, so that the training procedure cannot influence the “difficulty” of the produced perturbations. Our approach, which we call *ensemble adversarial training*, augments the training data with adversarial examples produced not only from the model being trained, but also from other *pre-trained* models. Including adversarial examples from external models during training removes the ability of the learning procedure to influence the nature of adversarial examples it is asked to classify. In particular, the degenerate optima discussed above no longer applies. As a by-product, ensemble adversarial training is also more closely tied with our original objective of defending against black-box attacks.

5.2 Experimental Setup

The models we use are given in Table 3. In each training batch, we rotate the source of adversarial examples between the model being trained and one of the pre-trained models. We recommend selecting the source model *at random* in each batch, to diversify perturbations across epochs. Gradients for the pre-trained models can be precomputed for the full training set. The per-batch cost of ensemble adversarial training is thus lower than that of standard adversarial training: using our method with $n - 1$ pre-trained models, only every n^{th} batch requires an extra forward-backward pass to compute an adversarial gradient. We evaluate robustness of trained models to black-box attacks by transferring adversarial examples crafted on a *separate holdout model, which was not used during training*.

MNIST: We train a new model, $A_{adv\text{-}ens}$, with the same architecture (A) and the same number of epochs (6) as model A_{adv} from Section 3.2. In each training batch of 64 inputs, we include 64 FGSM samples ($\epsilon = 0.3$), using either model A_{adv} or one of the external models A, C, D as the source.

ImageNet: We train two Inception v3 models and a Inception ResNet v2 model [17], using either two or three external pre-trained models. We use synchronous distributed training on 50 machines, with minibatches of size 16 (we did not pre-compute gradients, and thus lower the batch size to fit

Table 4: **Error rates (in %) for adversarial training and ensemble adversarial training on MNIST.** For the full test set, we report error rates on clean data, white-box FGSM ($\epsilon = 0.3$), and FGSM, I-FGSM ($\epsilon = 0.3, k = 10$) and RAND+FGSM ($\epsilon = 0.3, \alpha = 0.05$) samples transferred from the holdout model B. We compute 95% confidence intervals for a normal approximation of the mean test error and mark methods statistically tied for best in bold.

	Model	Clean	FGSM	FGSM_B	I-FGSM_B	RAND+FGSM_B
6 epochs	A_{adv}	1.0	3.6	18.2	19.8	12.4
	$A_{\text{adv-ens}}$	0.9	11.8	5.0	9.7	3.4
12 epochs	A_{adv}	0.7	3.8	15.5	13.5	9.5
	$A_{\text{adv-ens}}$	0.7	6.0	3.9	6.2	2.9

all pre-trained models into memory). Half of the examples in a minibatch are replaced by FGSM examples (targeted at the least likely class is according to the source model for that minibatch). As in [8], we use RMSProp with a learning rate of 0.045, decayed by a factor of 0.94 every two epochs.

5.3 Results

Results of all our experiments appear in Table 4 for MNIST, and Table 5 for ImageNet.

Convergence Speed. On MNIST, after 6 epochs of training, ensemble adversarial training greatly outperforms standard adversarial training on black-box attacks, but the error rate on white-box FGSM examples is still high ($A_{\text{adv-ens}}$ is trained on its own FGSM examples only every 4th batch). We thus train A_{adv} and $A_{\text{adv-ens}}$ for 6 additional epochs. Intuitively, more (standard) adversarial training will have little influence, as after 6 epochs the FGSM only produces “easy” perturbations and the adversarial loss is close to zero. In contrast, $A_{\text{adv-ens}}$ may benefit from additional training on “hard” perturbations computed on external models. Our experiments (see below) confirm this intuition.

We also observe slower convergence with ensemble adversarial training on ImageNet, probably as an inherent byproduct of training on “hard” adversarial examples. Kurakin et al. [8] report that after 187 epochs (150k iterations with minibatches of size 32), the $v3_{\text{adv}}$ model achieves 78% accuracy. In contrast, ensemble adversarial training for models $v3_{\text{adv-ens3}}$ and $v3_{\text{adv-ens4}}$ converges after about 280 epochs (450k iterations with minibatches of size 16). The Inception ResNet v2 model is trained for 175 epochs, where a baseline model reaches maximum accuracy at around 160 epochs.

Robustness to the FGSM. After 12 epochs on MNIST, model $A_{\text{adv-ens}}$ matches model A_{adv} on clean data, and vastly improves over it for FGSM samples transferred from the holdout model B. Robustness to white-box attacks is also significantly improved compared to the snapshot at 6 epochs.

On ImageNet, both Inception v3 models trained with ensemble adversarial training reach slightly lower accuracy on clean data, compared to non-adversarial training or standard adversarial training as in [8]. Although our models are more vulnerable to white-box FGSM samples compared to the $v3_{\text{adv}}$ model, ensemble adversarial training significantly increases robustness to black-box attacks that transfer FGSM samples crafted on the holdout Inception v4. Note that for $v3_{\text{adv-ens4}}$, the proportion of white-box FGSM samples seen during training is $\frac{1}{4}$ (instead of $\frac{1}{3}$ for model $v3_{\text{adv-ens3}}$). The negative impact on the robustness to white-box attacks is large, for only a minor gain in robustness to transferred samples. Results for the ResNet model are similar, although we did not train a model with standard adversarial training for this architecture. We observe a small loss in accuracy on clean examples and a significant increase in robustness to all attacks. For black-box FGSM samples, the loss in accuracy (compared to baseline accuracy on clean examples) is **4.8% (top 1)** or **2.0% (top 5)**.

In all cases, ensemble adversarial training removes the gradient masking effect (i.e., models are at least as robust to black-box FGSM attacks as to white-box attacks). We found the results to have little variance if we use a different holdout model as source of black-box attacks (we tried attacking the $v3_{\text{adv}}$ and $v3_{\text{adv-ens3}}$ models with an Inception ResNet v2 model), or if we use a smaller ϵ .

Robustness to Other Attacks. Ensemble adversarial training does not increase robustness to *white-box* I-FGSM and RAND+FGSM samples: the error rates are comparable to those for models A_{adv} on MNIST and $v3_{\text{adv}}$ on ImageNet, and omitted for brevity (see [8] for white-box I-FGSM attacks on

Table 5: **Error rates (in %) for adversarial training and ensemble adversarial training on ImageNet.** We report error rates on clean data and white-box FGSM ($\epsilon = 16/256$) over the full test set. For a random sample of 10,000 inputs from the test set, we report error rates on FGSM and RAND+FGSM (R+F) samples ($\epsilon = 16/256, \alpha = 8/256$) transferred from a holdout Inception v4 model. All attacks are targeted at the least-likely class. We mark methods statistically tied for best in bold, independently for both architectures (based on 95% confidence intervals).

Model	Top 1				Top 5			
	Clean	FGSM	FGSM _{v4}	R+F _{v4}	Clean	FGSM	FGSM _{v4}	R+F _{v4}
v3	22.0	69.8	43.8	42.8	6.1	42.8	18.9	17.4
v3 _{adv} [8]	22.0	26.8	36.5	30.8	6.1	9.0	13.5	10.4
v3 _{adv-ens3}	23.6	30.0	30.4	29.9	7.6	10.4	10.2	9.7
v3 _{adv-ens4}	24.2	43.1	29.6	29.1	7.8	19.5	9.6	9.5
IncRes v2	19.6	51.3	38.0	36.8	4.8	23.9	14.1	13.0
IncRes v2 _{adv-ens}	20.2	25.9	24.6	25.0	5.1	7.7	6.8	7.2

model v3_{adv} and Table 2 for white-box RAND+FGSM attacks). As conjectured in [8], larger models may be needed to attain robustness to such attacks. Yet, against black-box adversaries, these stronger attacks are only a concern insofar as they produce perturbations that reliably transfer between models.

On MNIST, we apply the I-FGSM and RAND+FGSM to the holdout model B and transfer the perturbed inputs to models A_{adv} and A_{adv-ens}. After 12 epochs of training, the adversarially trained model A_{adv} remains vulnerable to black-box attacks using either one-shot or iterative methods. Using ensemble adversarial training, we obtain far better robustness against all attacks.

For ImageNet, Kurakin et al. [8] showed that I-FGSM samples transfer at low rates, even between models trained without adversarial training. Thus, we focus on the RAND+FGSM here. We also find that the RAND+FGSM transfers at a lower rate than the FGSM (see the R+F column in Table 5). In summary, while ensemble adversarial training may not increase robustness to some classes of white-box attacks, we see an increase in robustness to *all types of black-box attacks* we considered.

6 Discussion and Future Work

Previous work on adversarial training has produced encouraging results, showing only a small gap in accuracy on clean versus (one-shot) adversarial examples [5, 8]. Yet, these results are misleading, as the adversarially trained models remain vulnerable to black-box attacks. With ensemble adversarial training, we significantly reduce the gap between white-box and black-box robustness. Although the resulting models are slightly less robust to some white-box attacks (compared to standard adversarial training), they fare much better against a more realistic and security-relevant black-box adversary.

We did not consider here *adaptive* black-box attackers that make use of queries to the target model’s prediction function (see Appendix A for a formal definition). Papernot et al. [13] use adaptive oracle queries to train a surrogate model for crafting adversarial examples. However, their attack is only effective if the adversary crafts perturbations with higher norm than those used in training the target model. If queries to the target model yield full *prediction confidences*, an adversary could estimate the target’s gradient at a given point using finite-differences (with 2d queries, i.e., over 130k queries on ImageNet), and fool the target with a RAND+FGSM attack. If queries only return the predicted label, the attack does not apply. Exploring stronger black-box attacks and evaluating their scalability to larger tasks is an interesting avenue for future work.

Our results, generic with respect to the application domain, suggest that the effectiveness of adversarial training can be improved by increasing the *diversity* of perturbations seen during training. A recent work by Baluja and Fischer hints at a conceptually similar but more computationally intensive idea [1]. They introduce *Adversarial Transformation Networks* (ATNs)—neural networks trained to produce adversarial examples for a particular target model—and suggest a variant of adversarial training that would train a model and an ATN in alternative fashion. Yet, it is plausible that ATNs would produce similar perturbations as with iterative methods, which do not currently seem amenable to adversarial training [8]. Iterative attacks and ATNs produce samples that transfer less [8, 1], so it is also unclear whether achieving robustness to these attacks would increase robustness to black-box attacks.

Acknowledgments

We thank Benedikt Bünz, Ian Goodfellow, Ben Poole and Jacob Steinhardt for helpful discussions. Nicolas Papernot is supported by a Google PhD Fellowship in Security. Research was supported in part by the Army Research Laboratory, under Cooperative Agreement Number W911NF-13-2-0045 (ARL Cyber Security CRA), and the Army Research Office under grant W911NF-13-1-0421. The views and conclusions contained in this document are those of the authors and should not be interpreted as representing the official policies, either expressed or implied, of the Army Research Laboratory or the U.S. Government. The U.S. Government is authorized to reproduce and distribute reprints for government purposes notwithstanding any copyright notation hereon.

References

- [1] Shumeet Baluja and Ian Fischer. Adversarial transformation networks: Learning to generate adversarial examples. *arXiv preprint arXiv:1703.09387*, 2017.
- [2] Battista Biggio, Igino Corona, Davide Maiorca, Blaine Nelson, Nedim Šrndić, Pavel Laskov, Giorgio Giacinto, and Fabio Roli. Evasion attacks against machine learning at test time. In *ECML-KDD*, pages 387–402. Springer, 2013.
- [3] Wieland Brendel and Matthias Bethge. Comment on " biologically inspired protection of deep networks from adversarial attacks". *arXiv preprint arXiv:1704.01547*, 2017.
- [4] Nicholas Carlini and David Wagner. Towards evaluating the robustness of neural networks. In *IEEE Symposium on Security and Privacy*, 2017.
- [5] Ian J Goodfellow, Jonathon Shlens, and Christian Szegedy. Explaining and harnessing adversarial examples. *arXiv preprint arXiv:1412.6572*, 2014.
- [6] Sergey Ioffe and Christian Szegedy. Batch normalization: Accelerating deep network training by reducing internal covariate shift. *arXiv preprint arXiv:1502.03167*, 2015.
- [7] Alexey Kurakin, Ian Goodfellow, and Samy Bengio. Adversarial examples in the physical world. In *ICLR*, 2017.
- [8] Alexey Kurakin, Ian Goodfellow, and Samy Bengio. Adversarial machine learning at scale. In *ICLR*, 2017.
- [9] Yanpei Liu, Xinyun Chen, Chang Liu, and Dawn Song. Delving into transferable adversarial examples and black-box attacks. In *ICLR*, 2017.
- [10] Seyed-Mohsen Moosavi-Dezfooli, Alhussein Fawzi, and Pascal Frossard. Deepfool: a simple and accurate method to fool deep neural networks. In *CVPR*, pages 2574–2582, 2016.
- [11] Aran Nayebi and Surya Ganguli. Biologically inspired protection of deep networks from adversarial attacks. *arXiv preprint arXiv:1703.09202*, 2017.
- [12] Alexander G Ororbia II, Daniel Kifer, and C Lee Giles. Unifying adversarial training algorithms with data gradient regularization. *Neural Computation*, 29(4):867–887, 2017.
- [13] Nicolas Papernot, Patrick McDaniel, Ian Goodfellow, Somesh Jha, Z Berkay Celik, and Ananthram Swami. Practical black-box attacks against machine learning. In *Asia Conference on Computer and Communications Security (ASIACCS)*, pages 506–519. ACM, 2017.
- [14] Nicolas Papernot, Patrick McDaniel, Somesh Jha, Matt Fredrikson, Z Berkay Celik, and Ananthram Swami. The limitations of deep learning in adversarial settings. In *Security and Privacy (EuroS&P), 2016 IEEE European Symposium on*, pages 372–387. IEEE, 2016.
- [15] Nicolas Papernot, Patrick McDaniel, Arunesh Sinha, and Michael Wellman. Towards the science of security and privacy in machine learning. *arXiv preprint arXiv:1611.03814*, 2016.
- [16] Nicolas Papernot, Patrick McDaniel, Xi Wu, Somesh Jha, and Ananthram Swami. Distillation as a defense to adversarial perturbations against deep neural networks. In *Security and Privacy (SP), 2016 IEEE Symposium on*, pages 582–597. IEEE, 2016.
- [17] Christian Szegedy, Sergey Ioffe, Vincent Vanhoucke, and Alex Alemi. Inception-v4, inception-resnet and the impact of residual connections on learning. *arXiv preprint arXiv:1602.07261*, 2016.

- [18] Christian Szegedy, Vincent Vanhoucke, Sergey Ioffe, Jon Shlens, and Zbigniew Wojna. Rethinking the inception architecture for computer vision. In *CVPR*, pages 2818–2826, 2016.
- [19] Christian Szegedy, Wojciech Zaremba, Ilya Sutskever, Joan Bruna, Dumitru Erhan, Ian Goodfellow, and Rob Fergus. Intriguing properties of neural networks. *arXiv preprint arXiv:1312.6199*, 2013.
- [20] Florian Tramèr, Nicolas Papernot, Ian Goodfellow, Dan Boneh, and Patrick McDaniel. The space of transferable adversarial examples. *arXiv preprint arXiv:1704.03453*, 2017.
- [21] Florian Tramèr, Fan Zhang, Ari Juels, Michael K Reiter, and Thomas Ristenpart. Stealing machine learning models via prediction apis. In *Usenix Security*, 2016.
- [22] Qinglong Wang, Wenbo Guo, II Ororbia, G Alexander, Xinyu Xing, Lin Lin, C Lee Giles, Xue Liu, Peng Liu, and Gang Xiong. Using non-invertible data transformations to build adversary-resistant deep neural networks. *arXiv preprint arXiv:1610.01934*, 2016.

A Threat Model: Formal Definitions

We provide formal definitions for the threat model introduced in Section 2.1. In the following, we make the parameters θ of an ML model f explicit by writing $f(x ; \theta)$. We consider a target model $f(\cdot ; \theta)$ trained over inputs (x, y_{true}) sampled from a data distribution μ . More precisely, we write

$$\theta \leftarrow \mathbf{train}(f, X_{\text{train}}, Y_{\text{train}}, r),$$

where \mathbf{train} is a *randomized training procedure* that takes in a description of the model architecture f , a training set $X_{\text{train}}, Y_{\text{train}}$ sampled from μ , and randomness r (e.g., for parameter initialization, dropout masks).

Given a set of test inputs $X \in [0, 1]^d$ (with labels Y) and a perturbation budget $\epsilon > 0$, an adversary \mathcal{A} produces a set of adversarial examples $X^{\text{adv}} \in [0, 1]^d$, such that for any $x, x^{\text{adv}} \in X \times X^{\text{adv}}$, we have $\|x - x^{\text{adv}}\|_\infty \leq \epsilon$. We evaluate success of the attack as the error rate of the target model over X^{adv} :

$$\frac{1}{|X^{\text{adv}}|} \sum_{(x^{\text{adv}}, y_{\text{true}}) \in X^{\text{adv}} \times Y} \mathbb{1}(f(x^{\text{adv}} ; \theta) \neq y_{\text{true}}).$$

We assume that \mathcal{A} can sample inputs according to the data distribution μ . We define three adversaries.

Definition 1 (White-Box Adversary). *For a target model $f(\cdot ; \theta)$, a white-box adversary is given access to all elements of the training procedure, that is \mathbf{train} (the training algorithm), f (the model architecture), the training data X, Y , the randomness r and the parameters θ . The adversary uses attacks such as those outlined in Section 2.2 to find adversarial inputs that maximize the model’s loss.*

White-box access to the internal model weights corresponds to a very strong adversarial model. We thus also consider the following relaxed and arguably more realistic notion of a *black-box* adversary.

Definition 2 (Non-Adaptive Black-Box Adversary). *For a target model $f(\cdot ; \theta)$, a non-adaptive black-box adversary only gets access to \mathbf{train} (the target model’s training procedure) and f (the model architecture). The adversary then chooses a procedure \mathbf{train}' and model architecture f' and trains a local model over samples from the data distribution μ . The adversary crafts adversarial examples X^{adv} on the local model f' using white-box attack strategies and applies these crafted inputs to the target model.*

Most importantly, a black-box adversary does not learn the randomness r used to train the target, nor the target’s parameters θ . The black-box adversaries in our paper are actually slightly *stronger* than the ones defined above, in that they use the same training data $X_{\text{train}}, Y_{\text{train}}$ as the target model.

We provide \mathcal{A} with the target’s training procedure \mathbf{train} to capture knowledge of *defensive strategies* applied at training time, e.g., adversarial training [19, 5] or ensemble adversarial training (see Section 5). The local training procedure \mathbf{train}' and model architecture f' chosen by the adversary may be different from those used to train the target.¹ In this work, we always mount black-box attacks that train a local model f' with a *different* architecture than the target model f . We actually find that black-box attacks on adversarially trained models are stronger when $f' \neq f$ (Table 1, Section 3).

¹ For ensemble adversarial training (see Section 5), \mathcal{A} also knows the architectures of all pre-trained models.

The main focus of our paper is on non-adaptive black-box adversaries as defined above. For completeness, we also formalize a stronger notion of *adaptive* black-box adversaries that additionally issue prediction queries to the target model [13].

Definition 3 (*Adaptive Black-Box Adversary*). *For a target model $f(\cdot; \theta)$, an adaptive black-box adversary only gets access to train (the target model’s training procedure) and f (the model architecture). The adversary issues (adaptive) oracle queries to the target model. That is, for arbitrary inputs $x \in [0, 1]^d$, the adversary obtains $f(x; \theta)$. The adversary then chooses a procedure train' and model architecture f' , trains a surrogate model over tuples (x, y) obtained from querying the target model, and uses this local model to craft adversarial examples.*

Papernot et al. [13] show that such attacks are possible even if the adversary only gets access to a small number of samples from μ . Note that if the target model’s prediction interface returns a measure of *prediction confidence* in addition to “hard” class labels, adaptive black-box adversaries could use queries to the target model to estimate the model’s gradient using finite differences, and then apply the attacks in Section 2.2. We further discuss adaptive black-box attack strategies in Section 6.

B Neural Network Architectures for MNIST

We train the following convolutional and fully-connected network architectures on MNIST.

Table 6: **Neural network architectures used in this work for the MNIST dataset.** Conv: convolutional layer, FC: fully connected layer.

A	B	C	D
Conv(64, 5, 5) + Relu	Dropout(0.2)	Conv(128, 3, 3) + Relu	$[\text{FC}(300) + \text{Relu}] \times 4$
Conv(64, 5, 5) + Relu	Conv(64, 8, 8) + Relu	Conv(64, 3, 3) + Relu	Dropout(0.5)
Dropout(0.25)	Conv(128, 6, 6) + Relu	Dropout(0.25)	FC + Softmax
FC(128) + Relu	Conv(128, 5, 5) + Relu	FC(128) + Relu	
Dropout(0.5)	Dropout(0.5)	Dropout(0.5)	
FC + Softmax	FC + Softmax	FC + Softmax	

C Different Forms of Gradient Masking

If adversarial examples did not transfer, a natural defense against gradient-based attacks such as the FGSM could consist in hiding information about the model’s gradient from the adversary. For instance, if the model is non-differentiable (e.g., a Decision Tree) or if the model’s gradient is zero at data points (i.e., the model is locally constant), gradient-based attacks are rendered ineffective. However, such defenses—referred to as “gradient masking” mechanisms in [15]—are unlikely to prevent black-box attacks. Below, we review two different types of gradient masking, gradient *hiding* and gradient *smoothing* that affect potential defenses against adversarial examples.

Given the prevalence of gradient masking in prior proposed defenses, we strongly encourage researchers to evaluate future defensive techniques in both white-box and black-box attack settings.

Gradient Hiding. Random Forests (RF) may seem ideal for preventing the attacks in Section 2.2: the models are non-differentiable and highly non-linear. Yet, RFs are easily fooled by transferring adversarial examples from a surrogate model: On MNIST, a RF of 100 trees achieves 97.1% accuracy on clean data, but FGSM examples ($\epsilon = 0.3$) crafted on a CNN transfer at a rate of 99%. Defenses based on preventing an adversary from computing the gradient have also been proposed [22]. We conjecture that such methods are unlikely to provide robustness against black-box attacks.

Gradient Smoothing. Defensive distillation [16] greatly reduces the effectiveness of white-box attacks by *smoothing out* the model’s gradient, leading to numerical instabilities in attacks such as the FGSM. Yet, distilled models were shown to be evadable via black-box attacks where adversarial examples are transferred from undefended models [13]. Moreover, Carlini et al. [4] show successful white-box attacks with simple modifications of the FGSM attack [4].

The saturated networks from [11] were found to perform a similar form of gradient masking [3] and are thus also likely vulnerable to black-box attacks.

D Other Hypotheses for Gradient Masking in Adversarial Training

In Section 3.3, we show that adversarial training exhibits gradient masking by modifying the curvature of the model’s loss function in the vicinity of data points. Here, we discuss two alternative hypotheses we investigated, for explaining why adversarial training may lead to gradient masking: (1) adversarial training *smooths out* the models gradient, similarly to defensive distillation [16]; or (2) adversarial training overfits on the specific type of adversarial examples encountered during training. However, we find neither of these hypotheses to be corroborated by our experiments.

Gradient Smoothing. Two proposed defenses against adversarial examples (Defensive Distillation [16] and Saturated Networks [11]) hinder first-order attacks (in part) by rendering gradient computations numerically unstable [4, 3]. These defenses can be evaded either through black-box attacks [13], or via simple modifications to the FGSM to account for small gradient magnitudes [4, 3].

Previous work has established connections between adversarial training and a form of regularization of the model’s gradient [5, 12]. Numerical instability of the gradient computation thus forms a natural hypothesis for the misleading robustness of adversarially trained models to white-box attacks. Yet, we find that adversarial training does not significantly smooth the gradient of the model’s loss.

We compute the average gradient magnitude $\frac{1}{n} \sum_{i=1}^n \|\nabla_x J(x, y_{\text{true}})\|_2$ over the full test set for models B and B_{adv} on MNIST, and the Inception v3 and $v3_{\text{adv}}$ models on ImageNet. The results appear in Table 7. On MNIST, adversarial training has a minor regularization effect on the gradients. However, on ImageNet, the average norm of the gradient *increases* with adversarial training.

Table 7: **Gradient norms with and without adversarial training.** Shows results on MNIST (left) and ImageNet (right) computed over the full test sets.

Gradient Norm	MNIST		ImageNet	
	A	A_{adv}	v3	$v3_{\text{adv}}$
mean	0.12	0.11	0.10	0.17
stdev	0.95	0.81	0.15	0.23

Overfitting. Adversarial training using a particular attack technique (e.g., FGSM) typically fails to significantly increase robustness to other attacks (e.g., iterative strategies) [8].² Another hypothesis to explain gradient masking when models are adversarially trained is that the defense “overfits” to the particular attack directions computed from the trained model. In other words, maybe the number of different adversarial perturbations is so large, that adversarial training successfully increases the model’s margins in adversarial directions that it sees (i.e., the ones given by the model’s gradient at each training point), but remains vulnerable to other unseen perturbations.

However, the overfitting hypothesis also fails to appropriately explain the vulnerability of adversarial training to black-box attacks. Indeed, even non-defended models tend to have large margins in the “adversarial” directions computed on the adversarially trained models. The results in Table 1 show that FGSM samples crafted on the adversarially trained models are easier to classify for all models. Thus, as argued in Section 3.3, it appears that adversarial training leads to models for which the FGSM mostly produces “easy” perturbations, although there exist other vulnerable directions.

E Transferability of RAND+FGSM Perturbations.

In Section 4, we introduce the RAND+FGSM attack, an extension of the original FGSM that prepends it with a small random perturbation. In Table 8, we evaluate the transferability of RAND+FGSM

² Kurakin et al. [8] note that iterative attacks tend to transfer at a much lower rate compared to non-iterative attacks. Thus, even if adversarial training does not substantially increase robustness to iterative attacks, the model may still be secure against black-box attacks.

adversarial examples on MNIST and ImageNet. Although the RAND+FGSM has a higher success rate than the FGSM in a white-box setting, it produces perturbations that transfer at a lower rate (see Table 1 for the same experiment using the FGSM).

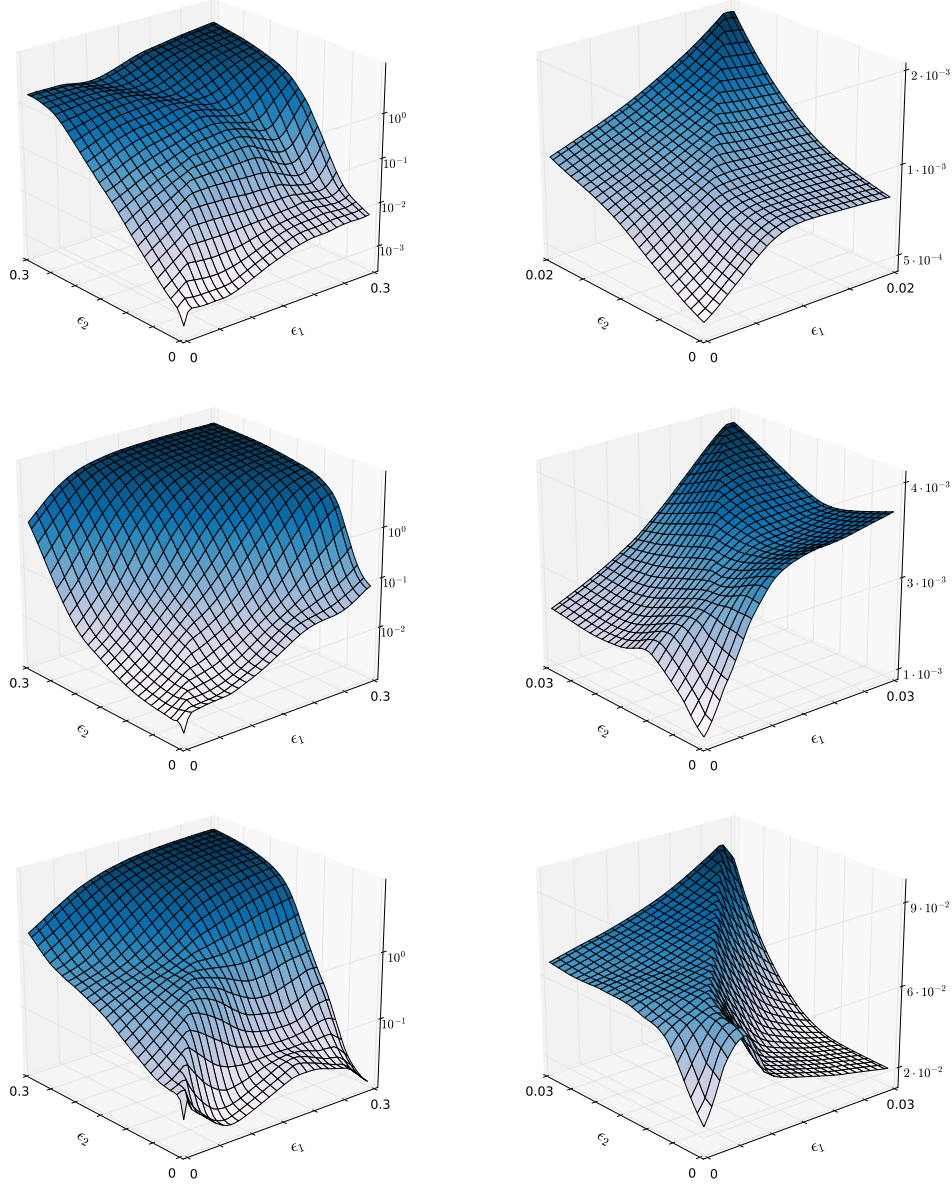
Table 8: Error rates (in %) of RAND+FGSM adversarial examples transferred between models. We use $\epsilon = 0.3, \alpha = 0.05$ for MNIST and $\epsilon = 16/256, \alpha = 8/256$ for ImageNet. Diagonal elements correspond to error rates for a white-box attack. Results on MNIST are computed over the full test set; results on ImageNet use a random sample of 10,000 inputs from the test set.

Source Model	Target Model			Source Model	Target Model			Source Model	Target Model		
	A	A_{adv}	B		v3	$v3_{adv}$	v4		v3	$v3_{adv}$	v4
A	75.3	10.0	53.1	v3	80.1	30.9	37.5	v3	57.7	10.4	14.3
A_{adv}	26.2	34.1	28.7	$v3_{adv}$	26.7	64.2	23.0	$v3_{adv}$	8.0	37.2	6.4
B	58.3	12.4	86.2	v4	42.8	30.8	70.3	v4	17.4	10.4	42.5

MNIST
ImageNet (top 1)
ImageNet (top 5)

F Illustrations of Loss Function Curvature with Adversarial Training

In Section 3.3, we show that adversarial training introduces spurious curvature artifacts in the model’s loss function around data points. As a result, one-shot attack strategies based on first-order approximations of the model loss produce perturbations that are non-adversarial. In Figure 3, we show further illustrations of this phenomenon for an adversarially trained model on MNIST.



(a) Loss surface for model A_{adv} (log-scale).

(b) Zoom in of the loss for small ϵ_1, ϵ_2 .

Figure 3: Additional illustrations of the local curvature artifacts introduced by adversarial training. The three data points are chosen such that the FGSM sample computed on the source model B (with $\epsilon = 0.3$) successfully transfers to model A_{adv} . For each data point, we plot the loss of model A_{adv} on samples of the form $x^* = x + \epsilon_1 \cdot \text{sign}(g_1) + \epsilon_2 \cdot \text{sign}(g_2)$, where g_1 is the gradient of model A_{adv} and g_2 is the gradient of model B. The right plots show the loss curvature close to the data points, and illustrate that the first-order approximation of the model’s loss is inaccurate for larger values of ϵ .